Structure of Active Phases during the Course of Electrocatalytic Reactions

ARTICLE *in* THE JOURNAL OF PHYSICAL CHEMISTRY B · JANUARY 2000

Impact Factor: 3.3 · DOI: 10.1021/jp9917446

2 AUTHORS, INCLUDING:

Jia Wang
Brookhaven National Laboratory
106 PUBLICATIONS **4,805** CITATIONS

SEE PROFILE

THE JOURNAL OF PHYSICAL CHEMISTRY B

 VOLUME 104, NUMBER 5, FEBRUARY 10, 2000

LETTERS

Structure of Active Phases during the Course of Electrocatalytic Reactions

R. R. Adžić* and J. X. Wang

Materials and Chemical Science Division, Department of Applied Science, Brookhaven National Laboratory, Upton, New York 11973

Received: May 26, 1999; In Final Form: November 3, 1999

Structures of ordered adsorbates have been determined during the course of the electrocatalytic reduction of oxygen by using synchrotron surface X-ray scattering techniques. The origin of the catalytic action of Tl adlayers on O_2 reduction on Au has been determined, and a possibility of measuring the adsorption configuration-specific activity in O_2 reduction has been demonstrated in the reaction on Ag(100) with Br adlayer. On the Au(111) electrode surface, the oxidation/redeposition of Tl in catalyzing the four-electron oxygen reduction is revealed from the analysis of X-ray diffraction intensity as a function of the O_2 reduction current for the $(3 \times \sqrt{3})$-2TlBr adlayer. This indicates that the redox property of the metal adsorbates is responsible for the catalytic effect. On Ag(100) with the c(2×2) Br adlayer, the O_2 reduction current resulting solely from adsorption in the "end-on" configuration through the 4-fold symmetry holes in the c(2×2) Br lattice is observed, showing that the "bridge" adsorption may not be necessary for the four-electron O_2 reduction on Ag at large overpotentials.

Introduction

Obtaining atomic scale information on the structure of the catalytic surface during the course of a reaction has been one of the major goals of studies in both heterogeneous catalysis and electrocatalysis. Such information can enhance our understanding of mechanisms of catalytic actions at surfaces and provide the basis for a rational approach to the design of new catalytic materials.[1,2] Studies under operating conditions are also important because of the often-observed reaction-induced surface restructuring,[2] and because they can reduce a gap between the "real world" and model catalytic systems.[1]

Scanning tunneling microscopy (STM) and atomic force microscopy (AFM) have been used to identify the active sites in catalytic[3] and electrocatalytic[4] reactions and to evaluate the reaction rate of atomically resolved surface processes.[5] These probes, however, have a limitation for observing surfaces under continuous reaction: the probing tip, approaching a surface at a distance of ~10 Å, can effectively block the supply of reactant to the part of the surface that is being scanned. Synchrotron radiation-based X-ray techniques, such as extended X-ray absorption fine structure spectroscopy (EXAFS) and X-ray absorption near-edge structure (XANES), have been used to study high surface area catalysts under reaction conditions yielding information on short-range atomic order, coordination numbers, and oxidation states. Here we demonstrate that detailed structural information on long-range ordered active phases can be obtained during the course of electrocatalytic reactions by using surface X-ray scattering (SXS) techniques. The same approach, mutatis mutandis, can be extended to various catalytic systems.

Electrocatalytic oxygen reduction is of utmost importance for electrochemical energy conversion in fuel cells and metal air batteries, corrosion, and several industrial processes. Consequently, it has attracted considerable attention over decades and

* Corresponding author.

10.1021/jp9917446 CCC: $19.00
Published on Web 01/15/2000

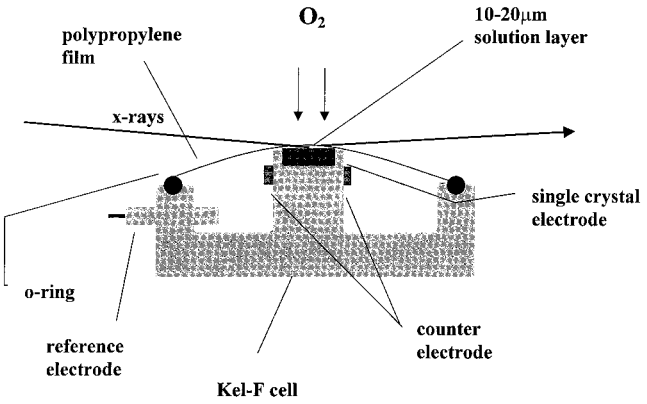

Figure 1. Simplified cross-section of the electrochemical and X-ray scattering cell used for determination of the electrode surface structure during the course of O_2 reduction.

continues to be a challenge because of its complex kinetics and the need for better electrocatalysts that support the vital four-electron reduction process.[6] Recent efforts in the fuel cells development have revived interest for improvement of the electrocatalysts for O_2 reduction. It is known that at low coverage Tl and Bi adlayers on Au support the four-electron reduction of O_2 to H_2O, viz., $O_2 + 4e^- + 4H^+ \rightarrow 2H_2O$, while a two-electron partial reduction, $O_2 + 2e^- + 2H^+ \rightarrow H_2O_2$, occurs on clean Au electrodes.[7] The mechanism of the catalytic action of these metal adsorbates is controversial. It may result from their specific electronic properties or from the formation of the bridge bond between O_2 and the Au−adatom sites, which facilitates the O−O bond scission.[8] Which of them plays the key role remained an open question partly due to the difficulty of obtaining structural information under operating conditions. In this work, we apply SXS to single-crystal electrode surfaces during the course of electrocatalytic O_2 reduction to identify the mechanism of catalytic action of Tl adatoms on Au(111) and to resolve the adsorption configuration-specific reactivities for the O_2 reduction on Ag(100). The results illustrate the unique features of the SXS techniques for studying surface catalytic mechanisms, and the conclusions may have significant impact on further search for efficient electrocatalysts for oxygen reduction.

Experimental Section

The electrochemical cell used for in situ SXS measurements is illustrated in Figure 1. A thin layer of electrolyte solution (10−20 μm thick) is maintained by surface tension between the front crystal face and the thin-film X-ray window when the cell is deflated during the measurements. Oxygen, the reactant, is brought into the cell through the gas-permeable X-ray window film. A continuous reaction condition is established by maintaining oxygen flow into the outer chamber fitted to the cell top (not drawn). Since the diffusion of oxygen through the film and the electrolyte layer is vertical to the crystal surface, the supply of the reactant is uniform across the sample area during the SXS measurements. The Au(111) crystal was flame-annealed and the Ag(100) crystal was polished chemically before each SXS and electrochemical measurement. A reversible hydrogen electrode (RHE) was used, and a pH-independent Ag/AgCl electrode was used in the pH = 10 solution (potentials are cited against NHE).

SXS measurements were carried out with focused monochromatic (λ = 1.2 Å) synchrotron radiation at the National Synchrotron Light Source at the ×22A beam line using a four-circle diffractometer in a vertical scattering geometry. The

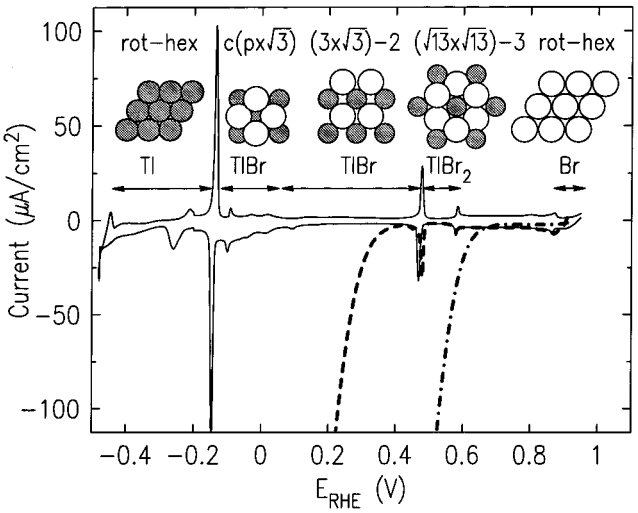

Figure 2. Current−potential curve obtained with the Au(111) electrode in 0.1 M $HClO_4$ solution containing 1 mM Tl^+ and 1 mM Br^- (solid line), and initial parts of cathodic going sweeps for O_2 reduction on the Au(111) in the solution containing Tl^+ and Br^- (dashed line) and containing Tl^+ only (dash−dot line). Sweep rates: 20 mV/s. Structures of previously reported ordered phases[9] are also shown, with open and shaded circles representing Br and Tl, respectively.

(*H*,*K*,*L*) coordinate system is hexagonal $a = b = 2.885$ Å, $c = 7.063$ Å, and tetragonal $a = b = 2.889$ Å, $c = 4.086$ Å for Au(111) and Ag(100), respectively, where *L* is along the surface normal direction. At grazing incident angle (∼1°), observed in-plane diffractions are indexed by (*H*,*K*). The intensities were measured by a NaI detector with the longitudinal in-plane resolution ranging from 0.01 to 0.02 $Å^{-1}$ (full width at half-maximum). The structure factors were obtained after correcting the integrated intensities for the variation of the Lorentz factor, the effective sample area, and the resolution along the surface normal direction.

Results and Discussion

Figure 2 shows a current−potential curve obtained in a linear potential sweep for the Au(111) electrode surface in 0.1 M $HClO_4$ containing 1 mM Tl^+ and 1 mM Br^-, and atomic models of five ordered phases determined by SXS in the absence of O_2. Structural determination of these phases in the absence of O_2 reduction has been reported elsewhere,[9] and a brief description is given below of the phases relevant to O_2 reduction. Sharp current peaks correspond to the structural phase transitions that separate the potential regions of five ordered adlayer phases. Two well-ordered coadsorbed phases with the $TlBr_2$ and TlBr stoichiometries and the unit cells ($\sqrt{13} \times \sqrt{13}$) and ($3 \times \sqrt{3}$), respectively, have distinctly different properties for O_2 reduction. In the ($\sqrt{13} \times \sqrt{13}$)-$TlBr_2$ phase, the lattice spacing between two adjacent hollow sites of the hexagonal Tl adlayer is smaller than the van der Waals diameter of Br. To accommodate the Br, half of the Br adions reside in a second layer, which is 3 Å above the first mixed adlayer, as revealed from the X-ray specular reflectivity measurements. The ($3 \times \sqrt{3}$)-2TlBr phase has a quasi-square symmetry that is typical for a binary ionic adlayer with opposite partial charges of similar quantity on the constituents. Both species are in the same plane and the nearest Tl−Br separation is close to the value in bulk TlBr crystal.

In the presence of oxygen, a large O_2 reduction current (Figure 2, dashed line) is observed at potentials negative of the current peak at 0.47 V. Rotating disk electrode measurements (not shown here) indicate that the reaction is a four-electron reduction

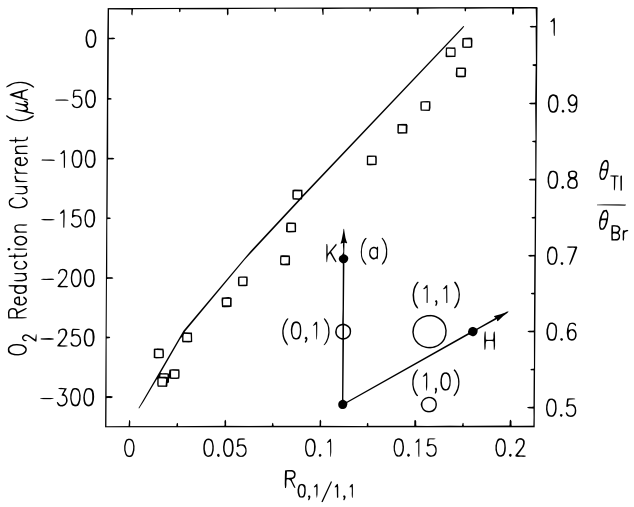

Figure 3. Positions of the low-order in-plane diffraction peaks from the Au(111) substrate (filled circles) and the $(3 \times \sqrt{3})$-2TlBr adlayer (open circles). The adlayer peaks are indexed using the primitive $(1.5 \times \sqrt{3})$ rectangular cell, and the areas of the open circles represent the structure factor intensities measured in the absence of O_2 (insert); O_2 reduction current (squres, left ordinate) as a function of the measured structure function intensity ratio, $R_{0,1/1,1}$, which is equal to $I_{(0,1)}/I_{(1,1)}$. The solid line shows the calculated $R_{0,1/1,1}$ (abscissa) as a function of the Tl/Br coverage ratio (right ordinate). Note that the current, not the current density, is used because the current density is not uniform across the crystal surface at large currents due to the edge effects. Thus, the correspondence between the Tl coverage and O_2 reduction current is not quantitative (see the text).

as in the Tl^+ solution without Br^-.[7] A comparison with the O_2 reduction on Au(111) with Tl adlayer without Br (Figure 2, dash−dot line) shows that the onset of reaction on the Au(111) with TlBr adlayer occurs at more negative potentials. The potential shift encompasses the potential region of the existence of the $(\sqrt{13} \times \sqrt{13})-3TlBr_2$ phase. In contrast to metal adsorbates, adsorbed Br is a known inhibitor of oxygen reduction. The inhibition effect of the $TlBr_2$ phase is probably caused by the Br adions in the second layer of the $TlBr_2$ phase that makes Tl less accessible to O_2 molecules.

Monitoring of the catalytic active $(3 \times \sqrt{3})$-2TlBr phase during the course of oxygen reduction was carried out by measuring the structure factors for its two low-order in-plane diffractions as a function of potential. As shown in Figure 3 (insert), the first-order peak at $(0,1)_{ad}$ is weaker than the second-order peak at $(1,1)_{ad}$. This is the characteristic of a mixed centered structure where the first- and second-order peaks have structure factors equal to the difference and the sum of the form factors of the two atomic species, respectively. In the absence of oxygen, the structure factor intensity ratio of these two peaks, $R_{0,1/1,1}$, remains constant at all potentials and agrees with the calculated value based on the $(3 \times \sqrt{3})$-2TlBr structure model. In the presence of oxygen and at potentials negative of the onset of oxygen reduction, the diffraction intensity at both positions, and more importantly, their intensity ratio, $R_{0,1/1,1}$, decrease with decreasing potential. This change can be directly related to the rate of O_2 reduction, measured as the cathodic current. As shown in Figure 3, the decrease of $R_{0,1/1,1}$ is nearly proportional to the increase of the reduction current. This relationship is also observed at a fixed potential when a mass transfer of O_2 is increased, which confirms that the change in $R_{0,1/1,1}$ is reaction-induced.

The measured $R_{0,1/1,1}$ can be correlated in a straightforward way to the coverage ratio of Tl to Br because $R_{0,1/1,1}$ is equal to $\exp(\sigma^2(q^2_{11} - q^2_{01}))\ (f_{Tl}\theta_{Tl} - f_{Br}\theta_{Br})^2/(f_{Tl}\theta_{Tl} + f_{Br}\theta_{Br})^2$, where σ, f, and θ are the root-mean-square displacement amplitude, the atomic factor and the atomic coverage, respectively. For $\theta_{Tl} = \theta_{Br}$, i.e., $\theta_{Tl}/\theta_{Br} = 1$, and $\sigma = 0.1$ Å, the calculated $R_{0,1/1,1}$ is 0.174, in good agreement with the value measured in the absence of O_2. Since Tl has a larger atomic factor than Br, $f_{Tl}\theta_{Tl} - f_{Br}\theta_{Br}$, and whence $R_{0,1/1,1}$, decrease as θ_{Tl}/θ_{Br} decreases. This is described by the solid line in Figure 3. By adjusting the scale of the coverage ratio (right ordinate), the calculated curve (solid line) can retrace the measured current vs $R_{0,1/1,1}$ curve (left ordinate). Thus, a semiquantitative relationship between the O_2 reduction current and the coverage ratio of Tl to Br is demonstrated.

The fact that Tl coverage decreases faster than Br coverage with increasing of the O_2 reduction current suggests that the partially charged Tl adatoms undergo oxidative desorption in catalyzing the four-electron reduction of O_2. The reaction is sustained because Tl adatoms are redeposited on the free lattice sites by the reduction of Tl^+. A similar mechanism involving a redox cycle for metal adsorbates has been proposed earlier,[10] but the lack of clear experimental evidence has left the question on the origin of the catalytic effect open. The SXS results described above provide a key experimental evidence for the oxidation/reduction of Tl, i.e., the redox property of Tl adatoms as the origin of their catalytic effect in oxygen reduction. The observed higher activity of the low coverage Tl phases for a four-electron O_2 reduction than that of the close-packed Tl phase can be explained with this mechanism. It appears that the Tl adatoms in low coverage phases are less stable than in a close-packed phase, and consequently more active in the redox cycle described above. The data obtained with a close-packed TlBr adlayer on Au(111) invalidate the mechanism which involves the formation of a bridge bond between O_2 and the Au−Tl sites since such a bonding is not possible on that surface. This corroborates the role of the redox property of the metal adatoms in catalyzing the O_2 reduction.

The current distribution in the electrochemical cell in Figure 1 is affected by the edge effects despite a direct supply of O_2 to the front surface. The rates of O_2 reduction are such that the effects are not significant. If the edge effects were considerable, a very good agreement between the experimental $R_{0,1/1,1}$ vs current plot and the calculated $R_{0,1/1,1}$ vs θ_{Tl}/θ_{Br} plot could not be obtained (Figure 3).

We also present results for O_2 reduction on Ag(100) to demonstrate that in situ monitoring of surface structure can reveal atomic processes for inert, stable adlayers that selectively block certain adsorption sites or adsorption configurations of molecules. An example of the latter case is given below which provides evidence for involvement of the “end-on" adsorption configuration of O_2 during the reduction on Ag(100) using the ordered Br adlayer to block the “bridge” adsorption.

Silver, in contrast to gold, supports a four-electron reduction of oxygen.[6] The “bridge” adsorption configuration has been assumed to be important for the four-electron reduction because the O−O bond splitting is more plausible when both oxygen atoms interact with the surface.[8] It is, however, difficult to verify the role of adsorption configuration in O_2 reduction. In our approach, an inert adlayer is utilized to block the “bridge” adsorption, hence, the O_2 reduction current can be solely related to the O_2 adsorption in the “end-on” configuration. The Ag(100)−Br system is ideal for this study because Br forms a well-ordered $c(2 \times 2)$ adlayer on Ag(100).[11] Through the 4-fold symmetry holes in the adlayer, O_2 molecules can reach the Ag surface in the “end-on”, but not in “bridge” adsorption config-

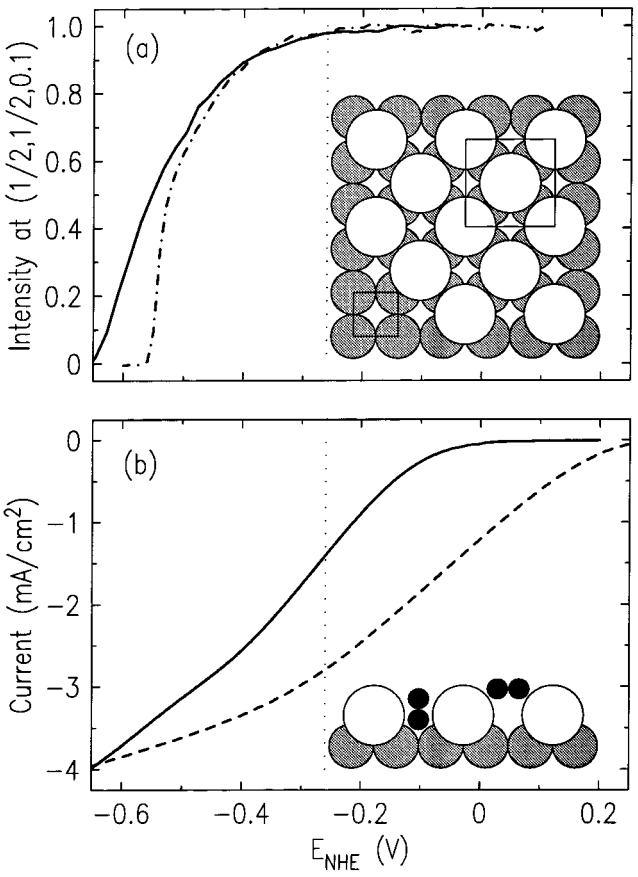

Figure 4. (a) Diffraction intensity at (1/2,1/2), after background subtraction, versus the applied potential in 0.1 M $NaClO_4$ (adjusted to pH = 10 by adding NaOH) containing 50 mM NaBr in the presence of N_2 (dash−dot line) and O_2 (solid line). Sweep rate 1 mV/s. In-plane structural model of the c(2 × 2) Br adlayer (open circles) on Ag(100) (shaded circles) is also shown. (b) Rotating disk hanging meniscus electrode measurements of the current−potential curves for O_2 reduction on Ag(100) in 0.1 M $NaClO_4$ (pH = 10) solution without Br^- (dashed line) and with 50 mM NaBr (solid line). Sweep rate 20 mV/s; 625 rpm. Vertical atomic model for "end-on" and "bridge" O_2 (solid circles) adsorption configuration on c(2 × 2) Br/Ag(100) is also given. The diameters of the circles are proportional to the diameters of the corresponding species. Oxygen molecules cannot reach Ag through the Br adlayer in a "bridge" configuration. The vertical dotted line marks the potential where the Ag(100) surface is completely covered by a c(2 × 2) Br adlayer and the O_2 reduction current is half of that in the absence of Br^-.

uration. This is illustrated by the structural models shown in Figure 4, where the diameters of the solid, shaded, and open circles are proportional to the diameters of O (1.20 Å), Br (3.90 Å), and Ag (2.89 Å), respectively.[12]

The potential region where a full c(2 × 2) Br adlayer exists in the presence of oxygen has been found to be the same as in its absence. This is shown in Figure 4a by the potential dependence of the diffraction intensity of the first-order adlayer peak at the (1/2,1/2) position. In the potential region where the (1/2,1/2) peak intensity is saturated, the Ag(100) surface is completely covered by a well ordered c(2 × 2) Br adlayer, as inferred from the resolution-limited peak width and the Br coverage obtained from analysis of the (0,1,*L*) intensity profile. In the X-ray electrochemical cell, the O_2 reduction current is observed negative of 0.0 V, while the decrease of the (1/2,1/2) diffraction intensity starts below −0.26 V. Therefore, the O_2 reduction takes place through the 4-fold symmetry holes in the c(2 × 2) Br adlayer at potentials between 0.0 and −0.26 V. The current becomes larger in the phase transition potential region where the c(2 × 2) phase vanishes. This current produces an uncompensated ohmic potential drop, which causes the diffraction intensity curve to extend to more negative potentials in the presence of oxygen than in its absence.

A certain increase of the solution pH can occur during O_2 reduction in this system. This cannot affect the measurements in any significant way since small reduction currents are observed in the presence of Br adlayer. The onset of O_2 reduction is shifted negatively by c(2 × 2) Br adlayer by 250 mV and, below this potential, the current is decreased because only half of the Ag sites are available for reaction (cf. Figure 4). Moreover, Br adsorption is not pH-dependent and the underlying silver cannot be oxidized at the potentials used, even if pH rose to 14. The oxidation of the Ag electrode would disorder the Br adlayer. This is not observed and the potential intervals of O_2 reduction in the X-ray diffraction cell agree well with the corresponding potentials observed in the rotating disk electrode measurements where pH change is avoided.

To measure the O_2 reduction current density accurately, rotating disk hanging meniscus electrode measurements have been carried out, and the results are shown in Figure 4b. On the adsorbate-free Ag(100) surface, oxygen reduction occurs below 0.25 V. In the presence of Br adsorption, the reduction current starts to increase below 0.0 V and reaches −1.4 mA/cm^2 at −0.26 V, which is approximately half of the current in the absence of Br^-. As shown in Figure 4a, Br forms a well-ordered c(2 × 2) adlayer above −0.26 V, which covers more than half of the surface area and allows O_2 molecules to reach the Ag electrode only through the "end-on" configuration. These facts suggest that adsorbed Br adlayer does not change the four-electron reduction pathway, otherwise, smaller current would be observed at −0.26 V. For a reaction involving a two-electron reduction to peroxide, the observed current would be half of that for bare Ag. Therefore, these measurements demonstrate that the "bridge" adsorption may not be necessary for a four-electron reduction of O_2 on Ag at large overpotentials.

Acknowledgment. The authors thank B. M. Ocko and S. Feldberg for useful discussions. This research was performed under the auspices of the U.S. Department of Energy, Divisions of Chemical and Materials Sciences, office of Basic Energy Sciences under Contract No. DE-AC02-98CH10886.

References and Notes

(1) Goodman, D. W. *J. Phys. Chem.* **1996**, *100*, 13090.

(2) Somorjai, G. A. *Introduction to Surface Chemistry and Catalysis*; Wiley-Interscience: New York, 1994; Chapter 7.

(3) Zambelli, T.; Wintterlin, J.; Trost, J.; Ertl, G. *Science* **1996**, *273*, 1688.

(4) Chen, C-h.; Gewirth, A. A. *J. Am. Chem. Soc.* **1992**, *114*, 5439.

(5) Wintterlin, J.; Volkening, S.; Janssens, T. V. W.; Zambelli, T.; Ertl, G. *Science* **1997**, *278*, 1931.

(6) Adžić, R. R. In *Electrocatalysis*; Lipkowski, J., Ross, P. N., Eds.; Wiley: New York, 1998; Chapter 5.

(7) Adžić, R. R.; Wang, J. X.; Ocko, B. M. *Electrochim. Acta* **1995**, *40*, 83.

(8) Yeager, E. B. *Electrochim. Acta* **1984**, *29*, 1527.

(9) Wang, J. X.; Robinson, I. K.; Adžić, R. R. *Surf. Sci.* **1998**, *412/413*, 374.

(10) McIntyre, J. D. E.; Peck, W. F. In *Proceedings of the Third Symposium on Electrode Processes*; Bruckenstein, S., McIntyre, J. D. E., Miller, B., Yeager, E. B., Eds.; The Electrochemical Society Inc.: Princeton, 1979.

(11) Ocko, B. M.; Wang, J. X.; Wandlowski, T. *Phys. Rev. Lett.* **1997**, *79*, 1511.

(12) Emsley, J. *The Elements*, 2nd ed.; Clarendon Press: Oxford, 1991.